

Quantum Hall states under conditions of vanishing Zeeman energy

F. J. Teran,^{1,2} M. Potemski,¹ D. K. Maude,¹ T. Andrearczyk,³ J. Jaroszynski,^{3,4} T. Wojtowicz,³ and G. Karczewski³

¹*Laboratoire National des Champs Magnétiques Intenses, CNRS-UJF-UPS-INSA, 38042 Grenoble, France*

²*Instituto Madrileño de Estudios Avanzados en Nanociencia,*

Ciudad Universitaria de Cantoblanco, 28049 Madrid, Spain

³*Institute of Physics, Polish Academy of Sciences, PL-02668 Warsaw, Poland*

⁴*National High Magnetic Field Laboratory, Tallahassee, Florida 32306, USA*

(Dated: November 9, 2018)

We report on magneto-transport measurements of a two-dimensional electron gas confined in a $\text{Cd}_{0.997}\text{Mn}_{0.003}\text{Te}$ quantum well structure under conditions of vanishing Zeeman energy. The electron Zeeman energy has been tuned via the $s-d$ exchange interaction in order to probe different quantum Hall states associated with metallic and insulating phases. We have observed that reducing Zeeman energy to zero does not necessarily imply the disappearing of quantum Hall states, *i.e.* a closing of the spin gap. The spin gap value under vanishing Zeeman energy conditions is shown to be dependent on the filling factor. Numerical simulations support a qualitative description of the experimental data presented in terms of a crossing or an avoided-crossing of spin split Landau levels with same orbital quantum number N .

PACS numbers: 71.10.Ca, 73.43.-f, 75.50.Pp

I. INTRODUCTION

In a quantizing magnetic field, the physics of a two-dimensional electron gas (2DEG) at very low temperatures is controlled by electron-electron interactions which dominate over the single particle physics leading to exotic collective ground states. For example, the spin exchange energy often dominates over the single particle Zeeman energy in the fractional and integer quantum Hall regimes.¹⁻²⁰ The rich physics of the quantum Hall ferromagnetism has attracted considerable interest when two spin split Landau levels with different spin index (*i.e.* σ) and orbital quantum number (N) are brought in coincidence.^{4,6,10,14,16-19} In this case, the quantum Hall effect (QHE) may exhibit hysteretic features with a complicated phenomenology^{16,18} related to phase transitions at non-zero temperatures. Such typical behavior of Ising ferromagnetic systems (*i.e.* with easy-axis anisotropy)¹⁴ can be explained in terms of domain walls¹⁴ or distinct symmetry-broken states¹⁵.

Equally, the crossing of spin split Landau levels with the same N and different spin index leads to interesting physics^{5,8,12}. In this case, QHE exhibits a different phenomenology related to no finite-temperature phase transitions without hysteretic features. Such typical behavior of Heisenberg ferromagnetic systems (*i.e.* isotropic anisotropy)¹⁴ leads to the existence of a non-zero electron spin gap in the energy spectrum of a 2DEG under conditions of vanishing Zeeman energy. This behavior has been observed in GaAs-based structures in the integer quantum Hall regime at $\nu = 1$ and 3. This could be explained as a consequence of the well established model^{2,3} of electron-electron exchange interaction (at least for $\nu = 1$) which forces a ferromagnetic ordering of the electronic spins at odd filling factors.^{5,8,12} Therefore, any small perturbation opens the electron spin gap (Δ_S) even when Zeeman energy is zero. Reasoning in

these terms also implies that the exchange contribution to Δ_S always dominates over the Zeeman term. This is in agreement with routine experimental observations in 2DEGs confined in III/V based structures which clearly show that Δ_S deduced from activated transport data at odd filling factors always greatly exceeds the single particle Zeeman energy.^{5,8,12} In addition, electronic spins cannot be treated as an isolated system but unavoidably interact with localized spins of nuclei²² or localized spins of substitutional magnetic ions, such as Mn^{2+} .^{18,23-26} The incorporation of localized magnetic moments in diluted magnetic semiconductors (DMS) offers unique spin splitting engineering³⁵ via the $s-d$ exchange interaction between the electron and magnetic ion spins²⁷. This can potentially be exploited to probe the spontaneous ferromagnetic order of a 2DEG via Δ_S when the electron Zeeman energy is continuously tuned through zero via the $s-d$ exchange interaction with localized spins.

Here, we report on the study of QHE in a n-type modulation doped $\text{Cd}_{0.997}\text{Mn}_{0.003}\text{Te}$ quantum well (QW) structure under conditions of vanishing Zeeman energy. So far, the standard method to tune the electron g-factor through zero in semiconductor structures was to apply hydrostatic pressure⁸. However, this method offers rather limited range of tunability of the Zeeman energy and can also modify the carrier density or the mobility. The incorporation of substitutional magnetic moments such as Mn^{2+} in CdTe QW structures offers an additional possibility of tuning the electron spin splitting via the $s-d$ exchange interaction between the spins of 2DEG and the localized magnetic moments²⁹. In a simple approach, the extended 2D electron and localised Mn^{2+} spins can be treated as two paramagnetic subsystems. Thus, a single electron spin feels the external magnetic field and the mean field resulting from the Mn^{2+} spin polarization. Due to the opposite signs of the bare Zeeman and $s-d$ exchange terms in a $\text{Cd}_{1-x}\text{Mn}_x\text{Te}$ QW, the

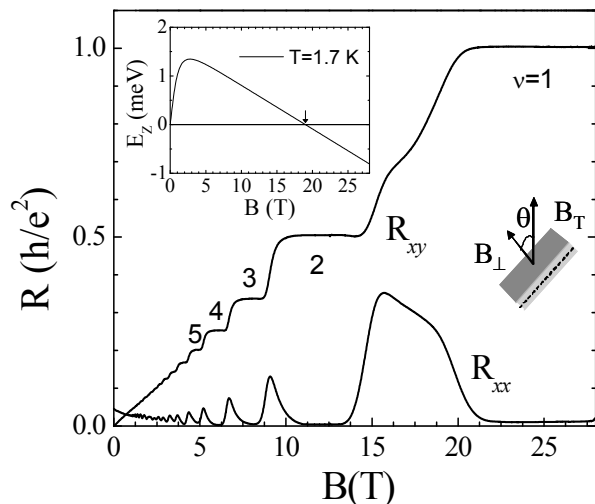


FIG. 1: (Color on line) Magnetic field dependence of R_{xx} and R_{xy} under perpendicular magnetic fields at $T = 1.7$ K for our sample with an electron density $n_e = 5.9 \times 10^{11} \text{ cm}^{-2}$. Left inset: Magnetic field dependence of E_Z at $T = 1.7$ K calculated according to Eq.1. Right inset: Schematic diagram indicating sample's orientation to magnetic field.

magnetic field (B) dependence of the total electron Zeeman energy (E_Z) results from the competition between these two contributions. At low magnetic fields where the $s-d$ exchange interaction term dominates, E_Z has large and positive values related to the $s-d$ exchange term. On increasing B , the bare Zeeman term increases linearly whereas the $s-d$ exchange interaction term saturates. Therefore, at high magnetic fields E_Z decreases because of the negative contribution related to the bare Zeeman term (see left inset of Figure 1). Thus, E_Z reaches zero value at a given magnetic field for which Zeeman term is equal to $s-d$ exchange term what depends on the Mn concentration. Thus, the particular B -dependence of E_Z in $\text{Cd}_{1-x}\text{Mn}_x\text{Te}$ QW structures allows to study the evolution of a given quantum Hall state when E_Z is continuously tuned from positive to negative values through zero. This can be achieved by simply tilting the plane of the 2D electron sheet with respect to the B -direction. That offers an unique opportunity to probe the ferromagnetic phenomenology of Heisenberg systems when the value of E_Z is modulated and the sign is inverted. The clear advantage of DMS systems is the wide range over which the g -factor can be continuously tuned without any changes in the mobility or carrier density. The disadvantage lies in the lower mobility (below $200.000 \text{ cm}^2\text{V}^{-1}\text{s}^{-1}$) of a 2DEG confined in magnetic QWs³⁶ with respect to their III-V non-magnetic counterparts. The experimental results presented in this work show that the condition of vanishing effective Zeeman energy in $\text{Cd}_{1-x}\text{Mn}_x\text{Te}$ QWs does not necessarily imply that Δ_S is zero. We also observe that the opening or closing of the Δ_S when $E_Z = 0$ tightly depend on the filling factor.

This paper is organized as follows. In Sec. II, we

present a description of the sample structure and the experimental procedure. In Sec. III, we show the magneto-transport data obtained from the tilted-field experiments, notably the evolution of longitudinal (R_{xx}) and transversal (R_{xy}) resistances as a function of E_Z and temperature for different filling factors. The R_{xy} shows the development of plateau between $\nu = 2$ and 1. This resistance feature is not associated with any quantum Hall state but rather related to the condition $E_Z = 0$. Moreover, the evolution of R_{xx} minima as the Zeeman energy passes through zero indicates that Δ_S remains open at $\nu = 3$ but closes at $\nu = 5$. In addition, the evolution of the R_{xx} maxima on either side of $\nu = 3$ (around $\nu = 7/2$ and $5/2$) under $E_Z = 0$ conditions is markedly different, suggesting a different opening of Δ_S . In Sec. IV, we present numerical simulations to qualitatively describe and discuss the Δ_S dependence on E_Z and B at distinct filling factors: $\nu = 3$ and 5 and $\nu = 7/2$, $5/2$ and $3/2$. Reasoning in terms of the density of states (DOS) at the Fermi level (E_F), we find two different situations which lead to distinct amount of DOS at the Fermi level ($DOS(E_F)$) under conditions of vanishing Zeeman energy. This depends upon whether the E_F lies inside either the upper or the lower spin level of a given spin split Landau level. Finally in Sec. V, we summarize the important points found in this work.

II. EXPERIMENTAL DETAILS

For the investigation, an n-type modulation doped structure made of a 10 nm thick $\text{Cd}_{1-x}\text{Mn}_x\text{Te}$ QW embedded between $\text{Cd}_{0.8}\text{Mg}_{0.2}\text{Te}$ barriers was employed. The effective Mn concentration in the QW is $x = 0.003$ determined from low magnetic field transport measurements²³. The 2DEG is formed by placing iodine doped n-type $\text{Cd}_{0.8}\text{Mg}_{0.2}\text{Te}$ layer separated from the $\text{Cd}_{0.997}\text{Mn}_{0.003}\text{Te}$ QW by 10 nm thick undoped $\text{Cd}_{0.8}\text{Mg}_{0.2}\text{Te}$ spacer. For the magneto-transport measurements a standard mesa etched Hall-bar was defined (typical dimensions 0.5×1 mm). The 2D electron concentration obtained from either the Hall resistance or the periodicity of the Shubnikov de Haas oscillations is $n_e = 5.9 \times 10^{11} \text{ cm}^{-2}$ and the mobility $\mu_e = 60.000 \text{ cm}^2\text{V}^{-1}\text{s}^{-1}$ at liquid helium temperatures. The sample was mounted on a rotation stage to tilt the sample with respect to magnetic field direction at temperatures (T) down to 50 mK and magnetic fields up to 28 T. The sample resistance components were measured using *ac* techniques (10.7 Hz with $I \sim 10 - 100$ nA). Whereas E_Z is defined by the total magnetic field (B_T), the filling factor is determined by the magnetic field component which is perpendicular to the 2D plane (B_\perp) (see right inset in Fig. 1). Thus, by rotating the sample the value of E_Z at a given filling factor is varied from positive to negative values passing through zero.

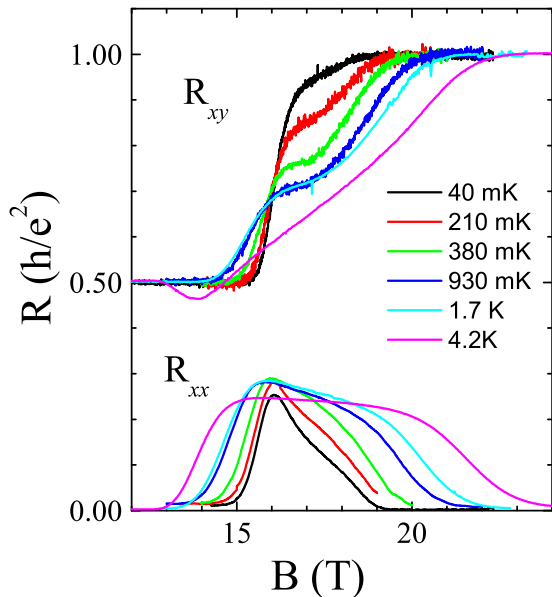


FIG. 2: (Color on line) Temperature dependence of R_{xx} and R_{xy} in the vicinity of $\nu = 3/2$.

III. MAGNETO-TRANSPORT RESULTS

A. Longitudinal and transverse resistance at perpendicular magnetic fields

Figure 1 shows the magneto-transport measurements of our sample under perpendicular magnetic fields up to $B = 28$ T at $T = 1.7$ K. A well developed Landau quantization at the integer quantum Hall regime is observed: well pronounced Shubnikov-de Haas oscillations in R_{xx} and quantized plateaus in R_{xy} . The rather broad R_{xy} plateaus associated to low filling factors (for instance, $\nu = 1$ and 2) and the low 2DEG mobility reveal the presence of relevant disorder in our sample. At low B (where $E_Z \geq \hbar\omega_c$), Shubnikov de Haas oscillations show complex beating patterns which have been discussed in detail in our previous work.²³ At higher B (where $\hbar\omega_c > E_Z$), both R_{xx} and R_{xy} show a typical QHE for a spin polarized 2DEG: resistance plateaus and minima associated with a continuous sequence of odd and even integer filling factors. However, certain R_{xx} and R_{xy} irregularities appear in the range of $B = 14 - 22$ T. At these magnetic fields, the R_{xx} maxima between $\nu = 2$ and 1 is anomalously distorted so that the development of an additional minimum in R_{xx} could be envisaged around $B = 17$ T. In parallel, a kink, resembling the development of quantum Hall plateau, is observed in the R_{xy} trace. These anomalies have been previously related to the appearance of the $\nu = 4/3$ fractional quantum Hall state³³. However, the T -dependence of R_{xy} and R_{xx} , shown in Figure 2,

rules out such a possibility. While there is some evidence for the existence of a plateau at intermediate temperatures (ranging 210 mK - 1.7 K), the feature washes out at the lowest temperatures rather than fully developing as expected for a fractional state. Indeed, the value of the anomalous plateau tightly depends on temperature: whereas at the lowest temperature ($T=40$ mK), the R_{xy} anomalous plateau almost reaches the value of h/e^2 , the value drops to $0.5h/e^2$ at the highest T (4.2K). The non-quantization of the developing plateau is a strong indication that an alternative explanation to fractional states should be sought. Simultaneously, the R_{xx} maxima broadens when increasing temperature. In order to clarify if the vanishing of E_Z is related to these resistance anomalies, we model the B and T -dependence of E_Z in our sample by assuming that:

$$E_Z = g_e \mu_B B + E_{s-d} \mathbb{B}_{5/2}(B, T, T_0) \quad (1)$$

where $g_e = -1.6$ is the electron g-factor in CdTe²⁸, μ_B is the Bohr magneton, $E_{s-d} = 1.25$ meV is the $s-d$ exchange interaction term between free electron and localized Mn^{2+} determined here from the low magnetic field transport measurements²³, $\mathbb{B}_{5/2}(B, T, T_0)$ is the modified Brillouin function, and T_0 is the effective temperature of the Mn spin subsystem²⁷ considering the magnetization correction due to the antiferromagnetic Mn^{2+} - Mn^{2+} interactions. In our particular sample, $T_0 = 0.12$ K was determined from transport measurements at low magnetic fields.²³ The expected B -dependence of E_Z in our sample at $T = 1.7$ K is shown in the inset of Fig.1. At low magnetic fields, E_Z has large and positive values related to the exchange term. Once the exchange term is saturated, E_Z decreases linearly with magnetic field and crosses zero around $B \sim 19$ T, *i.e.*, in the magnetic field range in which the R_{xx} and R_{xy} anomalies are observed.

In order to probe the relationship between the R_{xy} and R_{xx} anomalies associated to $\nu = 3/2$ and the $E_Z = 0$ condition, we have performed tilted-field magneto-transport experiments shown in Figure 3. The resistance anomalies observed at $B = 19$ T weaken when tilting the sample, *i.e.* when the $E_Z = 0$ condition is shifted towards lower B_{\perp} : the R_{xx} high field shoulder decreases and the R_{xy} non-quantized plateau significantly increases its value. This strongly suggests that those resistance anomalies observed between $B = 14 - 24$ T are related to the vanishing of E_Z which occurs in this magnetic field range as shown at the left inset of Fig.1.

To further elucidate the influence of a vanishing Zeeman energy on the magneto-transport properties, we have investigated the influence of tuning the Zeeman energy on integer quantum Hall states. At integer filling factors and low temperatures, our 2DEG shows zero resistivity and zero conductivity ($\rho_{xx} = \sigma_{xx} = 0$) indicating the existence of a well developed gap. Characteristically for insulating systems, the gap can be determined by thermally activated transport measurements. This procedure yields reliable gap values for clean 2DEG¹²

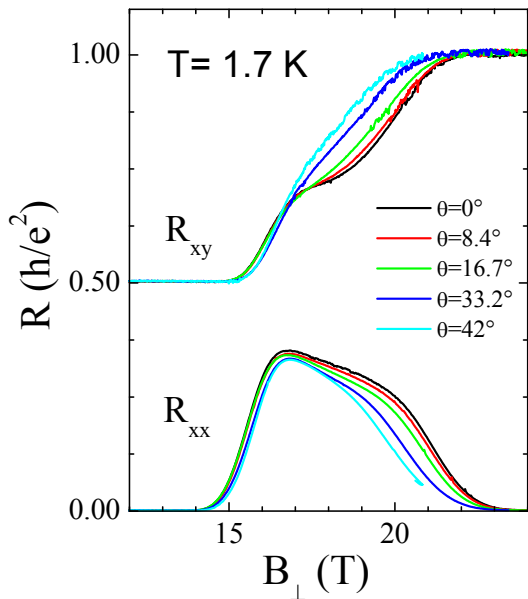


FIG. 3: (Color on line) R_{xx} and R_{xy} as a function of perpendicular magnetic fields, B_{\perp} , for different tilted angles θ in the vicinity of $\nu = 3/2$.

(*i.e.* narrow Landau level broadening). However, this is not the case for our 2DEG as revealed by the wide R_{xy} plateaus observed in Fig.1 and the low carrier mobility. Such plateau broadening can be related to the intrinsic disorder associated with ternary compounds, to the long range disorder associated with iodine donor impurities and/or with the presence of background dopants in the QW region. In a first approach, all these disorder mechanisms increase Landau level broadening leading to a large number of localized states. Nevertheless, thermally activated gaps obtained by T -dependence measurements in our sample may provide a qualitative evolution of Δ_S when tuning E_Z at given filling factor. Thus, we investigate the evolution of R_{xx} when Zeeman energy vanishes at $\nu = 3$ and 5 (insulating-like quantum Hall states). Furthermore, we similarly study the evolution of R_{xx} when the vanishing Zeeman energy is brought into coincidence with $\nu = 7/2$, $5/2$, and $3/2$ (metallic-like quantum Hall states).

B. Spin gaps at $\nu = 3$ and 5 versus Zeeman splitting

Figure 4 shows the R_{xx} measured in the T -range between 90 and 900 mK and at a fixed tilted angle $\theta = 63.8^\circ$. At this particular angle, vanishing Zeeman energy (*i.e.* $E_Z = 0$) and $\nu = 3$ coincide at $B_{\perp} = 8.1$ T. Under this condition, a well defined R_{xx} minimum is observed, reaching zero value below 200 mK. This clearly indicates that Δ_S at $\nu = 3$ remains open even under vanishing Zeeman energy conditions. Assuming a thermally activated behavior, the measured value of the resistance minima (R_{xx}^{min}) at $\nu = 3$ can be described by the following ex-

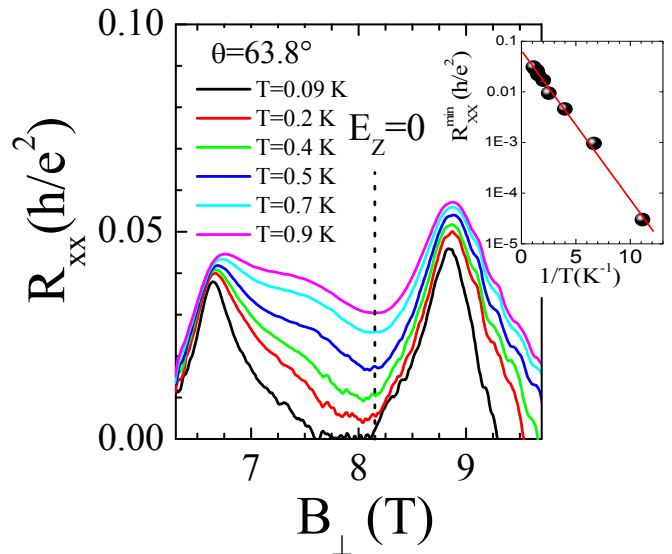


FIG. 4: (Color on line) Temperature dependence of R_{xx} minima related to $\nu = 3$ for a tilted angle $\theta = 63.8^\circ$ for which $E_Z = 0$ is expected at $B_{\perp 0} = 8.1$ T. Inset: Arrhenius plot of the T -dependence of R_{xx} at $B_{\perp 0} = 8.1$ T.

pression:

$$R_{xx}^{min} = R_0 \cdot \exp(-E_A/2kT) \quad (2)$$

a plot of $\ln(R_{xx}(T))$ versus $1/T$ allows us to deduce an activation energy $E_A = 0.25$ meV with the pre-factor $R_0 = 0.1h/e^2$ (see inset of Fig.4). In case of a dirty 2DEG, E_A should be increased by the width of the region of extended states (Γ_{ext}) in order to obtain a better estimate of spin gap¹². Thus, $\Delta_S = E_A + \sqrt{2}\Gamma_{ext}$. Simulations of R_{xx} at low fields were performed to model the magneto-transport measurements for our 2DEG system²³ considering $\Gamma_{ext} = 0.2$ meV. This value of Γ_{ext} is in agreement with the value of Landau level broadening ($\Gamma_{ext} = 0.075$ meV) employed in numerical simulations described in Section IV. Hence, we obtain a value of $\Delta_S = 0.53$ meV at $\nu = 3$ under conditions of vanishing Zeeman energy.

Figure 5(a) shows the evolution of R_{xx} when the $E_Z = 0$ condition is tuned through $\nu = 3$ at a fixed temperature. At $\theta = 0^\circ$, R_{xx} shows a well developed minima at $\nu = 3$ which becomes less pronounced when tilting the sample. At $\theta = 63.9^\circ$, the conditions $E_Z = 0$ and $\nu = 3$ coincide. At that angle, the value of R_{xx} at $\nu = 3$ shows a maximum. In contrast, R_{xx} at $\nu = 3$ recovers minimum values at larger angles (see data at $\theta = 72^\circ$). From Eq.1, we obtain the expected perpendicular magnetic field ($B_{\perp 0}$) for which $E_Z = 0$ at a given angle as indicated in the Figure 5. As expected, the R_{xx} minimum associated with $\nu = 3$ becomes less pronounced as E_Z is initially decreased when the sample is rotated away from the normal configuration. In contrast, the resistance minimum at $\nu = 3$ shows its maximum value

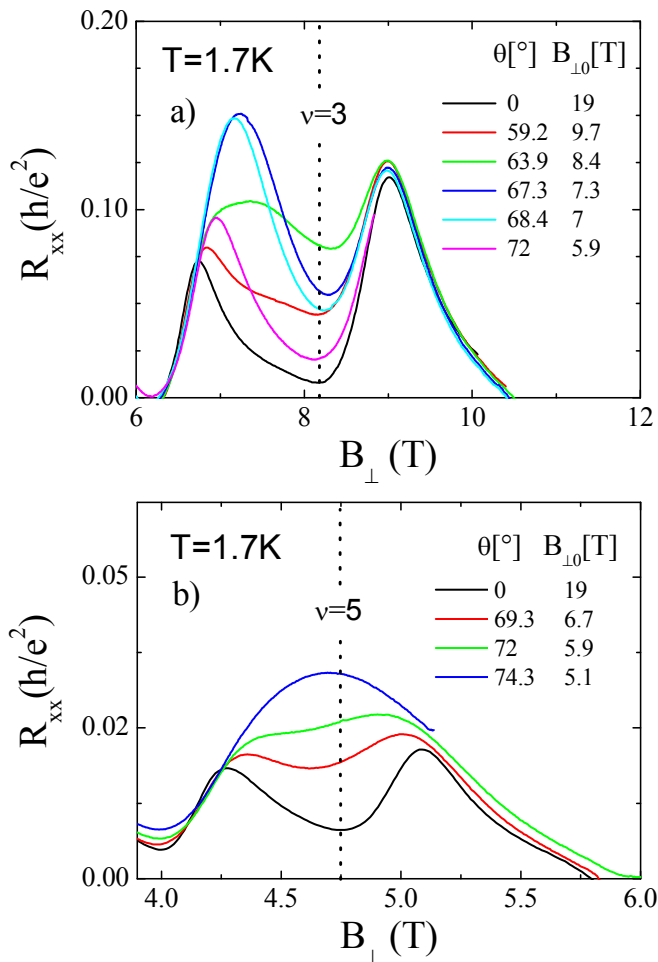


FIG. 5: (Color on line) (a) R_{xx} as a function of perpendicular magnetic field B_{\perp} for different tilt angles θ in the vicinity of $\nu = 3$ at $T = 1.7$ K. (b) R_{xx} as a function of perpendicular magnetic field B_{\perp} for different tilt angles θ in the vicinity of $\nu = 5$ at $T = 1.7$ K. The perpendicular magnetic field ($B_{\perp 0}$) for which $E_Z = 0$ is indicated for each angle.

when $E_Z \approx 0$. Afterwards, the resistance minimum at $\nu = 3$ decreases again for large tilt angles when E_Z large and negative values.

The results of similar measurements around $\nu = 5$ are quite different (see Fig.5(b)). The R_{xx} minimum is transformed into a maximum under vanishing Zeeman energy conditions. This indicates that, at least for the measurement temperature employed ($T = 1.7$ K), Δ_S collapses under conditions of vanishing Zeeman energy. Characteristically, a perfect overlap for the $N = 2$ spin split Landau levels when $E_Z \sim 0$ transforms the R_{xx} minima at $\nu = 5$ into a maximum whose amplitude is approximately twice that of the adjacent resistance maxima at $\nu = 11/2$ and $9/2$. The factor of two can be roughly understood assuming that R_{xx} is proportional to $DOS(E_F)^{31}$, which indeed approximately doubles when two spin Landau levels overlap. Finally, we have not found any evidence of hysteretic resistance traces around $\nu = 3$ and 5 quan-

tum Hall states at the temperature studied ($T = 1.7$ K). Assuming a thermally activated behavior from Eq.(1), the measured value of R_{xx} minima at $\nu = 3$ for a fixed temperature (Fig.5(a)) can be used to determine E_A as follows:

$$E_A(E_Z) = 2kT(-\ln(R_{xx}^{min}) + \ln(R_0)) \quad (3)$$

where $R_0 = 0.1h/e^2$ obtained from Arrhenius plot under $E_Z = 0$ at $\nu = 3$ conditions as mentioned above. The value of E_A was determined using Eq.(2), for a large number of angles (*i.e.* different E_Z values at $\nu = 3$) and six different temperatures ranging between 1.3 and 3.2 K. Figure 6 shows $\Delta_S = E_A + \sqrt{2}\Gamma_{ext}$ as a function of E_Z . The values of Δ_S determined from data taken at different temperatures all collapse onto the same curve which validates our assumption of a thermally activated behavior. As expected, Δ_S has a minimum value, $\Delta_S = 0.53$ meV, for a tilt angle $\theta \approx 64^\circ$ where $E_Z = 0$ in agreement with the Δ_S value obtained from fitting Eq.1 shown in the inset of Fig.4. Such a Δ_S value under vanishing Zeeman energy conditions seems extremely small in comparison to values of spin gap enhanced by electron-electron interactions. As mentioned above, the large Landau level broadening associated to this dirty 2DEG may lead to imprecise gap values from thermally activated measurements in the studied temperature range. However, it is enough to provide a qualitative description of the Δ_S dependence on E_Z . Thus, Figure 6 indicates that at $\nu = 3$, $\Delta_S \geq E_Z$ and clearly remains open when $E_Z = 0$. Either side of $E_Z = 0$, Δ_S increases linearly with E_Z but with different slopes, slightly steeper in the positive E_Z range than in the negative one. Such specific character of the Δ_S slopes may be related to the different behavior of R_{xx} maxima either sides of $\nu = 3$ when E_Z is tuned (see Fig.5(a)). Inspecting Fig.6, we notice that $\Delta_S \geq |E_Z|$ when $|E_Z|$ is sufficiently large. On the other hand, $\Delta_S \gg |E_Z|$ only when $E_Z \approx 0$. Reasoning in terms of spin split Landau levels, such characteristic dependence can be related to the effect of resonant level repulsion. We assign this phenomenon to electron-electron interaction related to electron spin polarization at $\nu = 3$. However as mentioned above, it is important to note that the opening of Δ_S in terms of resonant repulsion (avoided crossing) of spin split $N = 1$ Landau levels is not exactly what one would expect from the accepted knowledge of the physics of a 2DEG at odd filling factors in high quality III-V nanostructures. For a disorder free two-dimensional electrons, we would expect Δ_S to be the sum of the Zeeman energy and the electron-electron exchange energy, E_{e-e} , which is constant for a given filling factor and independent of the Zeeman energy. This would imply that $\Delta_S = E_{e-e} + E_Z$ which is not reflected in our experimental data (see dotted line in Fig.6). A model of spin Landau level repulsion (*i.e.* avoided crossing) is shown to successfully explain our observation as will be described in Section IV.

We summarize this section by pointing out the contrasting observation of the avoided crossing of spin Lan-

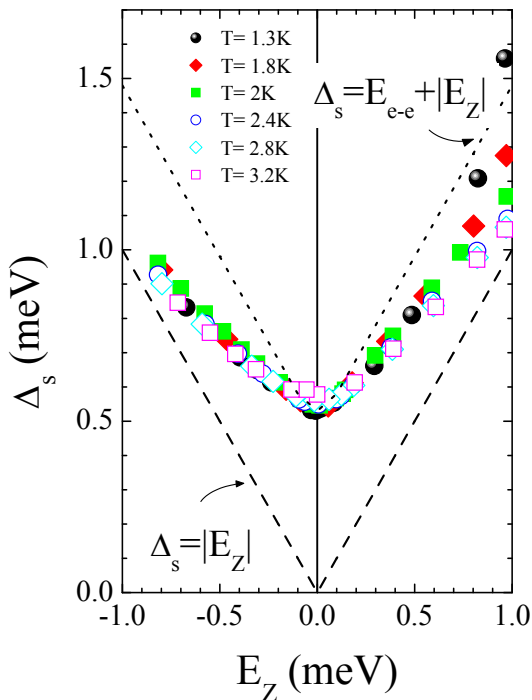


FIG. 6: (Color on line) Spin gap (Δ_S) as a function of Zeeman energy at $\nu = 3$ for different temperatures. Δ_S was obtained by using Eq.(2) as explained in the text. The dotted line represents the spin gap dependence $\Delta_S = E_Z + E_{e-e}$ and the dashed line $\Delta_S = E_Z$.

dau levels at $\nu = 3$ while a crossing of spin Landau levels is observed at $\nu = 5$.

C. Vanishing Zeeman splitting at half integer filling factors ($\nu = 7/2, 5/2$ and $3/2$)

We now turn our attention to the behavior of R_{xx} under vanishing Zeeman energy conditions when E_F lies in the center of a Landau level, *i.e.* metallic states, at $\nu = 7/2$ ($B_{\perp} \sim 6.6$ T), $\nu = 5/2$ ($B_{\perp} \sim 9$ T) and $\nu = 3/2$ ($B_{\perp} \sim 19$ T). The traces of R_{xx} at $T = 1.7$ K and different tilt angles shown in Fig.5(a) allow us to follow the evolution of the R_{xx} maxima at $\nu = 5/2$ and $7/2$ when E_Z is tuned through zero in the range $+1$ to -1 meV. The behavior of the $\nu = 5/2$ and $7/2$ R_{xx} peaks is significantly different. The position and amplitude of the resistance maximum associated with $\nu = 5/2$ remains independent of the effective Zeeman energy. In contrast, R_{xx} maximum associated with $\nu = 7/2$ is strongly influenced by E_Z . As E_Z is decreased at $\nu = 7/2$ by tilting the sample, the $\nu = 7/2$ R_{xx} maxima broadens (see data measured at $\theta = 59.2^\circ$) on the high magnetic field side and its amplitude increases. At $\theta = 67.3^\circ$, the sample is under conditions of $E_Z = 0$ at $\nu = 7/2$. In this situation, the amplitude of the R_{xx} maximum related to $\nu = 7/2$ is roughly twice the value at $\theta = 0^\circ$. At larger tilt angles, E_Z is increasingly negative leading to the recovery

of R_{xx} trace observed at $\theta = 0^\circ$. Assuming that R_{xx} is proportional to the $DOS(E_F)$, it is intuitively clear that the doubling of the R_{xx} maximum can be interpreted as a result of a double degeneracy (perfect overlap) of spin-split $N = 1$ Landau levels. We consider that the effect of the R_{xx} increase can be seen as a characteristic feature indicating some overlap of the otherwise spin split $N = 1$ Landau levels. An unchanged resistance would correspond to a situation in which the $DOS(E_F)$ remains unchanged and therefore Δ_S remains open, which is the case observed for the $\nu = 5/2$ R_{xx} maximum. In terms of our model of “repulsing levels”, we deduce that spin split $N = 1$ Landau levels may cross at $\nu = 7/2$ while they avoid to cross at $\nu = 5/2$. We have found no evidence of hysteretic resistance traces around $\nu = 7/2$ and $5/2$ quantum Hall states at the temperature range studied.

Turning back to the tilted-field behavior of the R_{xx} peak around $\nu = 3/2$, we note that this case is a mixing of the $\nu = 5/2$ and $7/2$ cases. As shown in Fig.3, the amplitude of the R_{xx} peak observed around $\nu = 3/2$ is essentially not affected by tilting the sample as in case of $\nu = 5/2$. In contrast, the high field side of R_{xx} peak narrows when tilting the sample as shown for $\nu = 7/2$ large angles ($\theta > 67.3^\circ$) where E_Z increases. Simultaneously, the R_{xy} plateau disappears. This particular behavior can be interpreted as the result of a slight overlap between the spin split $N = 0$ Landau levels at $B_{\perp} \sim 19$ T which diminishes by tilting the sample (*i.e.* increasing E_Z). The slight overlap can be interpreted as an avoided crossing of spin split $N = 0$ Landau levels under vanishing Zeeman energy conditions. Numerical simulations presented in next Section IV will qualitatively support this interpretation.

We summarize this section by pointing out the observation of the avoided crossing of spin Landau levels at $\nu = 5/2$ and $3/2$ in contrast with the observed crossing of spin Landau levels at $\nu = 7/2$.

IV. NUMERICAL SIMULATIONS

In order to qualitatively account the directly visible consequences of different Δ_S values on the magneto-transport properties of the 2DEG, we have performed numerical calculations. In the following section, we develop a simple model which phenomenologically introduces the spin splitting in terms of an energy of interaction for the avoided crossing of the spin split Landau levels. The model is capable of qualitatively reproducing the experimental data and gives some insight into the evolution of Δ_S with E_Z and filling factor. In order to do that, we assume different interaction terms depending on filling factor. In addition, we assume that the total density of the electronic states under magnetic field can be described by a set of Gaussian broadened Landau levels. The energy of an electron under quantizing magnetic fields which interacts with Mn^{2+} ions within a single particle picture is given by:

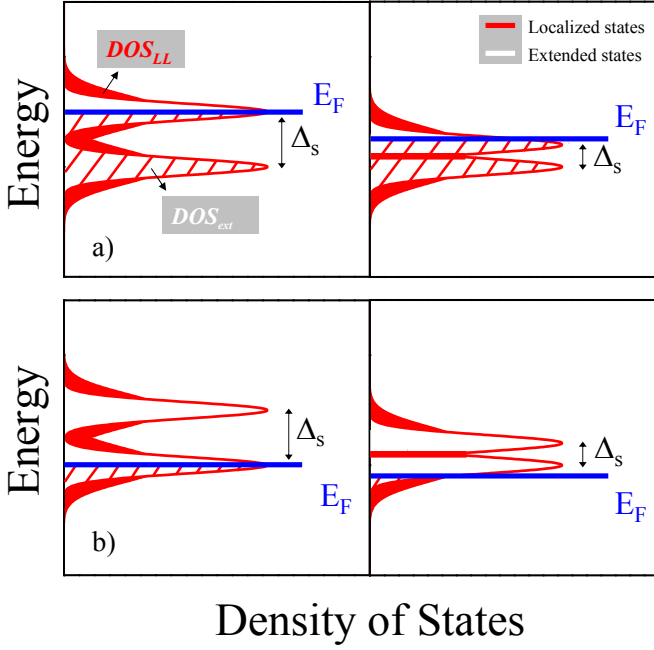


FIG. 7: (Color on line) Schematic illustration of the Gaussian DOS_{LL} and DOS_{ext} with widths Γ_{LL} and Γ_{ext} , respectively, in two different conditions of Landau level mixing (right side: mixing, left side: no mixing) when E_F lies a) in spin-up Landau level (as in case of $\nu = 3/2$ and $7/2$) and b) spin-down Landau level (as in case of $\nu = 5/2$).

$$E_{N,\sigma} = (N + 1/2)\hbar\omega_c + E_Z\sigma \quad (4)$$

where $N = 0, 1, 2, \dots$ corresponds to the Landau level index, σ denotes the electron angular momentum whose z-component has the value $+1/2(-1/2)$ for spin up(down), $\hbar\omega_c = eB_{\perp}/m_e^*$ denotes the cyclotron energy and $m_e^* = 0.107 m_o$ is the electron effective mass determined by cyclotron resonance³⁰. E_Z is given by Eq.1. In addition, the DOS of spin resolved Landau levels with Gaussian broadening is described as

$$DOS_{LL} = \sum_{N,\sigma} \frac{eB}{h} \frac{1}{\Gamma_{LL}\sqrt{2\pi}} \exp\left(-\frac{(E - E_{N,\sigma})^2}{2\Gamma_{LL}^2}\right) \quad (5)$$

where Γ_{LL} is the Landau level Gaussian broadening parameter. We neglect the effective thermal distribution when calculating E_F assuming $T = 0$ K for electrons. The procedure of calculating R_{xx} and R_{xy} distinguishes between localized and extended states³¹ as shown in Fig.7. The calculation procedure considers that only the latter ones contribute to the conductivity. In order to do that, we assume that in the central part of each Landau level there exists a band of extended states of Gaussian form whose DOS is given by

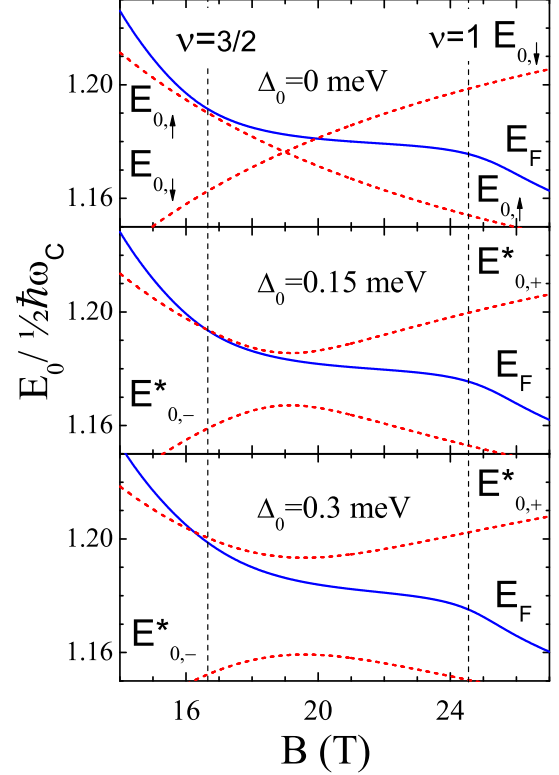


FIG. 8: (Color on line) The calculated E_F (solid line) and energy of the spin split $N = 0$ Landau levels normalized to $1/2\hbar\omega_c$ (dotted lines) as a function of magnetic field for different values of Δ_0 and $T = 1.7$ K.

$$DOS_{ext} = \sum_{N,\sigma} \frac{eB}{h} \frac{1}{\Gamma_{ext}\sqrt{2\pi}} \exp\left(-\frac{(E - E_{N,\sigma})^2}{2\Gamma_{ext}^2}\right) \quad (6)$$

where $\Gamma_{ext} < \Gamma_{LL}$. For a given perpendicular magnetic field, E_F is calculated numerically by integrating over the total density of states³¹ (*i.e.* DOS_{LL}). R_{xx} is then taken to be proportional to the density of extended states at E_F , *i.e.* $DOS_{ext}(E_F)$ and R_{xy} is proportional to the integral of R_{xx} .³¹ Our experimental data show that the spin gap remains open even under vanishing E_Z conditions. In order to reproduce such a behavior, we assume that spin split Landau levels with index N , $E_{N\uparrow,\downarrow}$, are replaced by interacting levels $E_{N+,-}^*$ to calculate DOS_{LL} and DOS_{ext} . The energy levels $E_{N+,-}^*$ for $N=0$ are given by

$$E_{0+,-}^* = \frac{1}{2}(E_{0\uparrow} - E_{0\downarrow}) \pm \left\{ \frac{1}{4}(E_{0\uparrow} - E_{0\downarrow})^2 + \left(\frac{\Delta_0}{2}\right)^2 \right\}^{1/2} \quad (7)$$

where $\Delta_0/2$ is the energy of interaction for the avoided

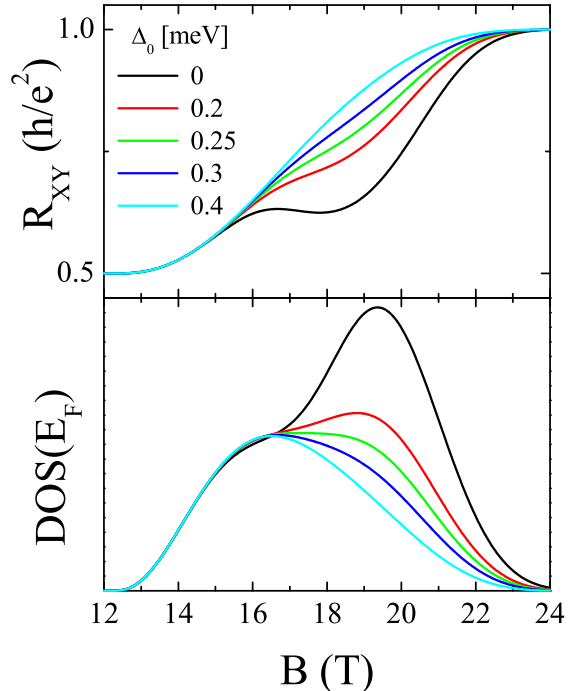


FIG. 9: (Color on line) Calculated R_{xy} and $DOS(E_F)$ as a function of magnetic field for different values of Δ_0 and $T = 1.7$ K.

crossing. Physically, Δ_0 corresponds to the experimentally observed spin gap Δ_S under vanishing Zeeman energy conditions (*i.e.* when $E_Z = 0$).

The adjustable parameters in our simulations are; the total width of the Landau level (Γ_{LL}), the width of the band of the extended states (Γ_{ext}) and the interaction parameter Δ_0 . We have found that our data are best described when $\Gamma_{LL} = 0.15$ meV and $\Gamma_{ext} = 0.075$ meV both assumed to be constant in the magnetic field range considered ($B = 4 - 28$ T). The value of Γ_{LL} corresponds to a scattering time $\tau = 2.75 \times 10^{-11}$ s in reasonable agreement with the transport scattering time $\tau_t \approx 3.65 \times 10^{-11}$ s deduced from the sample mobility. On the other hand, the interaction parameter Δ_0 was found to be dependent on magnetic field as will be described below.

A. Vanishing spin gaps at half integer filling factors ($\nu = 7/2, 5/2$ and $3/2$)

Initially, we focus our attention on modeling the resistance anomalies observed near $B \sim 19$ T at $\nu = 3/2$ (see Fig.2). The non-quantized R_{xy} plateau and the high-field shoulder of R_{xx} can be understood due to the floating up of E_F when the spin split $N = 0$ Landau

levels approach under vanishing Zeeman energy conditions. This is tightly related to $DOS(E_F)$. The description of $DOS(E_F)$ depends on the value of Δ_0 as can be seen in Fig.8. There, we represent traces of the calculated evolution the spin split $N = 0$ Landau levels and E_F as a function of magnetic field for different values of Δ_0 and $T = 1.7$ K (required to calculate E_Z). When $\Delta_0 = 0$ meV, the spin split $N = 0$ Landau levels cross at $B \sim 19$ T. E_F goes slightly above the crossing of spin split $N = 0$ Landau levels leading to an additional peak of the $DOS_{ext}(E_F)$ and a pronounced broadening as shown in Figure 9; at the same time a kink appears in R_{xy} which resembles a plateau development (see in Fig.9). When increasing Δ_0 value till 0.2 meV, the $DOS(E_F)$ reduces when E_F goes through the center of the upper spin branch Landau level (see Fig.8) over a wide range of magnetic fields. The E_F behavior with respect to spin split Landau levels gives rise to broad and pronounced $DOS_{ext}(E_F)$ peak around $B = 19$ T but with a smaller amplitude than in case of $\Delta_0 = 0$ meV. Simultaneously, the R_{xy} kink increases its resistance value around $B = 19$ T with respect to $\Delta_0 = 0$ meV (see Fig.9). In contrast, for larger Δ_0 values (0.25 – 0.4 meV), the spin split $N = 0$ Landau levels have a more pronounced energetic distance leading to a significant reduction of $DOS(E_F)$ when E_F goes from $E_{0,+}$ towards $E_{0,-}$. The increase of magnetic field raises the degeneracy of the Landau levels pulling down E_F with respect to the center of the upper spin branch (see Fig.8). This is reflected in the transport properties as a transformation of the $DOS_{ext}(E_F)$ peak into a high field shoulder which becomes less pronounced as Δ_0 further increases (see Fig.9). Simultaneously, the R_{xy} kink continuously increases its resistance value and become less pronounced when increasing Δ_0 (see Fig.9).

In addition, the effect of tilting the sample can be reasonably modeled for $\nu = 3/2$ by considering $\Delta_0 = 0.3$ meV. As shown in Figure 10, the simulation qualitatively reproduces our observations fairly well (compare with Fig.3): the value of the R_{xy} plateau increases with the tilt angle θ , reaching the value of the adjacent integer quantum Hall plateau (*i.e.* h/e^2) for $\theta > 33^\circ$. At this tilted angle, the R_{xy} trace shows a unique slope while for smaller angles two different slopes can be appreciated, in good agreement with the experimental data (see 3). Simultaneously, the R_{xx} maximum become narrower exclusively on the high field side when tilting the sample. At the same time the shoulder shifts to lower B_\perp and becomes less pronounced, qualitatively in good agreement with experiments. In our simulations, the behavior of E_F depends on a single parameter which is the ratio of the interaction energy to the Landau level broadening (Δ_0/Γ_{LL}) so that the determined value of Δ_0 depends on the Landau level broadening used. Another important limitation of the model corresponds to the description of the T -dependence of the plateau. In a first approach, we may expect that increasing temperature the number of localized states should decrease.³² This may therefore

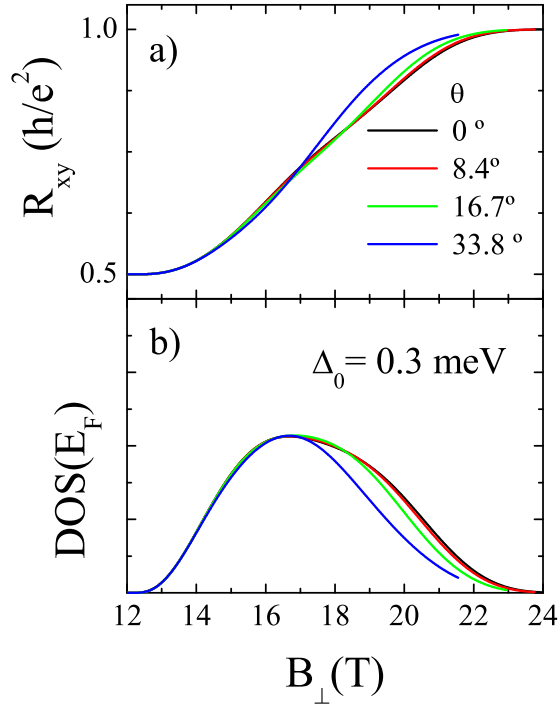


FIG. 10: (Color on line) Calculated R_{xy} and $DOS(E_F)$ as a function of magnetic field for different tilt angles in the vicinity of $\nu = 3/2$ for $\Delta_0 = 0.3$ meV and $T = 1.7$ K.

affect the plateau formation and also the broadening of the R_{xx} minima associated with $\nu = 1$ as we clearly see in Fig.2. In our calculations, changing Δ_0 should lead to similar effects which is not the case (see Fig.9).

Our model qualitatively describes the R_{xy} anomaly as the result of an avoided crossing of spin split $N = 0$ Landau levels which slightly overlap under vanishing Zeeman energy conditions for a given Δ_0/Γ_{LL} ratio. In the standard picture of the integer QHE, the quantization of Hall plateaus is assigned to electron localization. Moving away from integer filling factors, the electron density and their localization length increases. Hence, free electrons become delocalized leading to the increase of R_{xy} because the plateau quantization is lost. Thus, we may expect a non-quantized plateau when Landau level cross under vanishing Zeeman energy condition. This particular circumstance related to the mixing of localized-delocalized states at the Fermi level when $E_Z = 0$ (see Fig.7) originates the reentrant of an insulating phase responsible of the observation of a non-quantized plateau. Under such spin Landau level mixing conditions, the thermal activation determines the value of the R_{xy} as shown in Fig.2. Reasoning in similar terms, this model also explains the appearance of the R_{xx} high field shoulder at $\nu = 3/2$. The success of our qualitative model represents an important goal which allows to predict the appearance of

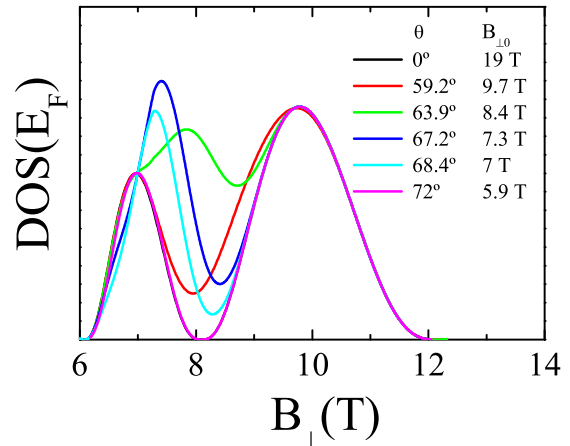


FIG. 11: (Color on line) Calculated $DOS_{ext}(E_F)$ as a function of magnetic field in the vicinity of $\nu = 3$ considering $\Delta_0 = f(B_{\perp})$ and $T = 1.7$ K as described in the text. The perpendicular magnetic field for which $E_Z = 0$ ($B_{\perp 0}$) is noted for each angle.

non-quantized plateaus each time Landau level crossing and E_F coincide. The important parameters which favor the observation of such resistance anomalies are Δ_0 and Γ_{LL} . The disorder favors the observations of such resistance phenomena: high-magnetic field R_{xx} shoulder (instead of well pronounced peaks) and well developed non-quantized R_{xy} plateau (instead of Delta function-like plateau reductions¹⁵). Moreover, our observations reveals that, at the temperature range studied, the crossing (or avoided crossing) of Landau levels with the same N and different σ index does not lead to hysteretic resistance behaviour, contrary to the case with different N and σ indexes.^{15,18}

Although we conclude that spin Landau levels avoid to cross in both the $\nu = 3/2$ and $\nu = 5/2$ case, the corresponding R_{xx} resistance maxima behave quite differently when E_Z is varied: high field shoulder disappearing at $\nu = 3/2$ and no changes at $\nu = 5/2$. We think, this "asymmetry" results from the fact that partial overlap of spin Landau levels affects the position of E_F in a different way depending on whether E_F is located in the vicinity of the upper or of the lower spin level. Our reasoning is schematically illustrated in Fig.7. The situation when E_F is in the vicinity of the upper spin level, which, for example, corresponds to the case of a 2DEG at $\nu = 3/2$, is considered in Fig.7(a). In Fig.7(b), E_F is in the vicinity of the lower spin level which, for example, illustrates the $\nu = 5/2$ case. In the left side panel of Fig.7 we consider well separated spin levels and the condition at which the maximum in the R_{xx} should occur (E_F located exactly at the center of the corresponding Landau level). Let us now imagine that we increase the magnetic field but

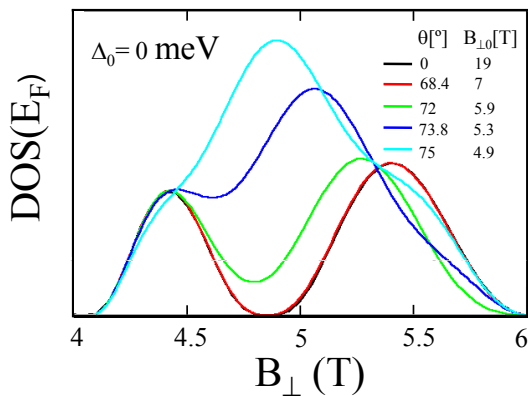


FIG. 12: (Color on line) Calculated extended $DOS(E_F)$ as a function of magnetic field in the vicinity of $\nu=5$ considering $\Delta_0 = 0$ meV and $T = 1.7$ K as described in the text. The perpendicular magnetic field for which $E_Z = 0$ ($B_{\perp 0}$) is noted for each plot.

at the same time the spin levels approach leading to a partial overlap. The primary effect of the increase of the magnetic field is to increase the Landau level degeneracy and therefore to lower E_F with respect to the center of the corresponding spin Landau level. This simply translates into a decrease of the corresponding resistance by assuming that $R_{xx} \sim DOS(E_F)$. However, as shown in Fig.7, the position of E_F (with respect to the center of the corresponding spin Landau level) is also affected by the increasing overlap of the spin levels. We note that the energy level overlap leads to the decrease of DOS available below the center of the upper spin level and to the increase of DOS below the center of the lower level. Therefore, increasing the overlap between spin levels we push E_F up if it is in the vicinity of the upper spin level and push it down if it is in the vicinity of the lower spin branch. We expect that the additional “overlap induced” downwards shift of E_F may somehow speed up the decay of the corresponding R_{xx} peak, but the effect of “overlap induced upwards shift” of E_F may have much more pronounced consequences on the observed shape of the corresponding R_{xx} maxima.

Therefore, we may qualitatively understand the effect of the broadening of the $\nu = 3/2$ resistance maximum observed on the high field side when separation between spin Landau levels becomes small. Even more severe distortions of this resistance peak could be expected, for example, the situation when E_F crosses twice the center of the same spin level and therefore the observation of the splitting of the $\nu = 3/2$ peak should be, in principle, possible. We show in the next section that our qualitative considerations are confirmed by a more quantitative approach to simulate numerically our experimental results.

B. Spin gaps at $\nu = 3$ and 5 versus Zeeman splitting

We now turn to the discussion of the shape of the R_{xx} traces obtained as the effective Zeeman energy is swept through zero in the range $4 < \nu < 2$ shown in Fig.5(a). We know that the gap at $\nu = 3$ and $\nu = 5/2$ remains open with a $\Delta_0 = 0.3$ meV. The doubling of the resistance peak at $\nu = 7/2$ under conditions of vanishing Zeeman energy suggests that Δ_S closes (*i.e.* $\Delta_0 \ll \Gamma_{LL}$). It is clear that there is a strong filling factor dependence of Δ_0 which rapidly changes from zero to finite values. A rapid opening of Δ_S is well known in GaAs based 2DEG’s and is generally explained in terms of the exchange energy which is proportional to the characteristic Coulomb energy and proportional to the spin polarization of the system. Since, for broadened Landau levels, the spin polarization depends on the size of Δ_S a positive feedback occurs and the onset of spin splitting is generally very abrupt. This can be modeled but requires that the gap and spin polarization be calculated self-consistently. We make the simplistic approximation that the residual gap depends only on the Coulomb energy so that $\Delta_0 \propto \sqrt{B}$. The calculated $DOS_{ext}(E_F)$ as a function of perpendicular magnetic field for different tilt angles and $T = 1.7$ K (required to calculate E_Z) are shown in Fig.11. Given the simplicity of the model used the agreement with the measured resistance (see Fig.5(a)) is reasonably good. As E_Z passes through zero the peak around $\nu \approx 7/2$ increases in amplitude and shifts to higher fields. To complete our simulations, we consider R_{xx} around $\nu = 5$ and show that it is possible to roughly reproduce the experimental results (see Fig.5.(b)). Assuming $\Delta_0 = 0$ and $T = 1.7$ K, our numerical simulations support the qualitative description of the experimental data concluding that spin Landau levels cross (*i.e.* perfect spin Landau level overlap) when $E_Z = 0$ leading to R_{xx} maxima, as shown in Figure 12.

V. SUMMARY

We have studied the evolution of quantum Hall states under conditions of vanishing Zeeman energy. The experimental results presented here show that the condition of vanishing effective Zeeman energy does not necessarily imply the closing of the spin gap. We observe that the opening or closing of the spin gap is a function of the filling factor. Thus, Δ_S remains closed for $\nu = 5$ and $7/2$ and opened for $\nu = 3, 5/2$ and $3/2$ at the temperature studied ($T=1.7$ K). Moreover, the experimental procedure allows the investigation of quantum Hall states under vanishing Zeeman energy conditions not only for insulating quantum Hall states (*i.e.* $\nu = 3$ and 5) but also for metallic states in the vicinity of $\nu = 3/2, 5/2$ and $7/2$. A phenomenological model based on an avoided crossing between the two spin split components of the corresponding Landau level qualitatively reproduce the R_{xx} and R_{xy} measurements at different conditions. Thus, we show

that the mixing of localized and delocalized states under avoided Landau level crossing conditions leads to the appearance of a non-quantized plateau in the R_{xy} . Our observations can be explained assuming that Δ_S evolves in terms of e-e interactions mediated by disorder leading to a different filling factor dependence.

VI. ACKNOWLEDGMENTS

This work has been supported by the Foundation for Polish Science through subsidy 12/2007, the European

Union through the EuroMagNET contract n° 228043 and the Innovative Economy grant POIG.01.01.02-00-008/08 related to the European Regional Development Fund.

-
- ¹ H. Cho, J. B. Young, W. Kang, K. L. Campman, A. C. Gossard, M. Bichler, and W. Wegscheider, Phys. Rev. Lett. **81**, 2522 (1998).
- ² Yu. A. Bychkov, S. V. Iordanskii, and G. M. Eliashberg, JETP Lett. **33**, 152 (1981).
- ³ C. Kallin and B. I. Halperin, Phys. Rev. B **31**, 3635 (1985).
- ⁴ R. J. Nicholas, R. J. Haug, K. von Klitzing and G. Weimann, Phys. Rev. B **37**, 1294 (1988).
- ⁵ A. Usher, R. J. Nicholas, J. J. Harris and C. T. Foxon, Phys. Rev. B **41**, 1129 (1990).
- ⁶ S. Koch, R. J. Haug, K. von Klitzing and M. Razeghi, Phys. Rev. B **47**, 4048 (1993).
- ⁷ A. Schmeller, J. P. Eisenstein, L. N. Pfeiffer and K. W. West, Phys. Rev. Lett. **75**, 4290 (1995).
- ⁸ D. K. Maude, M. Potemski, J. C. Portal, M. Henini, L. Eaves, G. Hill and M. A. Pate, Phys. Rev. Lett. **77**, 4604 (1996).
- ⁹ S. A. J. Wieggers, M. Specht, L. P. Levy, M. Y. Simmons, D. A. Ritchie, A. Cavanna, B. Etienne, G. Martinez and P. Wyder, Phys. Rev. Lett. **79**, 3238 (1997).
- ¹⁰ A. J. Daneshvar, C. J. B. Ford, M. Y. Simmons, A. V. Khaetskii, A. R. Hamilton, M. Pepper and D. A. Ritchie, Phys. Rev. Lett. **79**, 4449 (1997).
- ¹¹ T. Jungwirth, S. P. Shukla, L. Smrcka, M. Shayegan and A.H. MacDonald, Phys. Rev Lett. **81**, 2328 (1998).
- ¹² D. R. Leadley, R. J. Nicholas, J. J. Harris, C. T. Foxon, Phys. Rev. B **58**, 13036 (1998).
- ¹³ S. M. Girvin, Physics Today **53**, 39 (2000).
- ¹⁴ T. Jungwirth and A. H. MacDonald, Phys. Rev. B **63**, 035305 (2000).
- ¹⁵ H. J. P. Freire and J. C. Egues, Phys. Rev. Lett. **99**, 026801 (2007).
- ¹⁶ E. P. de Poortere, E. Tutuc, S. J. Papadakis and M. Shayegan, Science **290**, 1546 (2000).
- ¹⁷ K. Vakili, T. Gokmen, O. Gunawan, Y. P. Shkolnikov, E. P. de Poortere and M. Shayegan, Phys. Rev. Lett. **97**, 116803 (2006).
- ¹⁸ J. Jaroszynski, T. Andrearczyk, G. Karczewski, J. Wrobel, T. Wojtowicz, E. Papis, E. Kaminska, A. Piotrowska, D. Popovic and T. Dietl, Phys. Rev. Lett. **89**, 266802 (2002).
- ¹⁹ W. Desrat, F. Giazotto, V. Pellegrini, M. Governale, F. Beltram, F. Capotondi, G. Biasiol and L. Sorba, Phys. Rev. B **71**, 153314 (2005).
- ²⁰ F. Fischer, R. Winkler, D. Schuh, M. Bichler and M. Grayson, Phys. Rev. B **75**, 073303 (2007).
- ²¹ M. Dobers, K. von Klitzing, J. Schneider, G. Weiman and K. Ploog, Phys. Rev. Lett. **61**, 1650 (1988).
- ²² S. E. Barret, G. Dabbagh, L. N. Pfeiffer, K. W. West and R. Tycko, Phys. Rev. Lett. **74**, 5112 (1995).
- ²³ F. J. Teran, M. Potemski, D. K. Maude, T. Andrearczyk, J. Jaroszynski and G. Karczewski, Phys. Rev. Lett. **88**, 186803 (2002).
- ²⁴ R. Knobel, N. Samarth, J. G. E. Harris and D. D. Awschalom, Phys. Rev. B **65**, 235327 (2002).
- ²⁵ H. Buhmann, E. G. Novik, V. Daumer, J. Liu, Y. S. Gui, C. R. Becker and L. W. Molenkamp, Appl. Phys. Lett. **86**, 2104 (2005).
- ²⁶ Y. S. Gui, C. R. Becker, J. Liu, V. Daumer, V. Hock, H. Buhmann and L. W. Molenkamp, Europhys. Lett. **65**, 393 (2004).
- ²⁷ J. K. Furdyna, J. Appl. Phys. **64**, R29 (1988).
- ²⁸ A. A. Sirenko, T. Ruf, M. Cardona, D. R. Yakolev, W. Ossau, A. Waag and G. Landwehr, Phys. Rev. B **56**, 2114 (1997).
- ²⁹ F. J. Teran, M. Potemski, D. K. Maude, Z. Wilamowski, A. K. Hassan, D. Plantier, J. Jaroszynski, T. Wojtowicz and G. Karczewski, Physica E **17**, 335 (2003).
- ³⁰ M. L. Sadowski, F. J. Teran, M. Potemski, G. Karczewski, M. Kutrowski, J. Jaroszynski and T. Wojtowicz, in *Proc. 24th Int. Conf. on Physics of Semiconductors*, edited by D. Gershoni, (World Scientific, Singapore, 1995).
- ³¹ M. van der Burgt, V. C. Karavolas, F. M. Peeters, J. Singleton, R. J. Nicholas, F. Herlach, J. J. Harris, M. Van Hove and G. Borghs, Phys. Rev. B **52**, 12218 (1995).
- ³² L. B. Rigal, D. K. Maude, M. Potemski, J. C. Portal, L. Eaves, Z. R. Wasilewski, G. Hill and M. A. Pate, Phys. Rev. Lett. **82**, 1249 (1999).
- ³³
- ³⁴ F. J. Teran, M. Potemski, D. K. Maude, T. Andrearczyk, J. Jaroszynski and G. Karczewski, in *Proc. 25th Int. Conf. on Physics of Semiconductors*, edited by N. Miura and T. Ando, (World Scientific Publications, Springer-Verlag, Heidelberg, 2001), Vol. 2, p. 943.
- ³⁵ T. Wojtowicz, M. Kutrowski, G. Karczewski, J. Kossut, B. Koning, A. Keller, D. R. Yakolev, A. Waag, J. Geurts, W. Ossau, G. Landwehr, I. A. Merkulov, F. J. Teran, and M. Potemski, J. Cryst. Growth **214-215**, 378 (2000).
- ³⁶ V. Kolkovsky, M. Wiater, G. Karczewski, C. Betthausen, A. Vogl, D. Weiss and T. Wojtowicz, in Book of abstracts of the 5th International School and Conference on Spintronics and Quantum Information Technology, p. 77, July 7-11, Krakow, Poland, (2009).